5370 *Organometallics* **2000,** *19,* 5370−5375

Aufbau Approach to Multimetallic Ensembles Based on Tetrathiooxalate: $[Cp^*_4Rh_4(C_2S_4)_2]^{2+}$, $[Cp^*_3Rh_2Ru(C_2S_4)]^+$, and $[Cp^*_6Rh_6(C_2S_4)_2]^{4+}$

Geoffrey A. Holloway, Kevin K. Klausmeyer, Scott R. Wilson, and
Thomas B. Rauchfuss*

*School of Chemical Sciences, University of Illinois at Urbana−Champaign,
Urbana, Illinois 61801*

Received June 20, 2000

Experiments aimed at the characterization of new coordination modes for tetrathiooxalate (TTO) are described. Cyclic voltammetric (CV) measurements on $Cp^*_2Rh_2(C_2S_4)$ (**1**) revealed an irreversible oxidation as part of an ECE process that results in the chemically reversible dimerization of $\mathbf{1}^+$. Treatment of **1** with $CpFe[C_5H_4C(O)Me]BF_4$ followed by anion exchange gave $[Cp^*_4Rh_4(C_2S_4)_2](BPh_4)_2$, the dication of which consists of a dimer of $\mathbf{1}^+$ linked through two pairs of Rh−S bonds. A second new bonding mode for TTO was generated by treatment of **1** with $[Cp^*Ru(MeCN)_3]PF_6$ to give $[Cp^*_3Rh_2Ru(C_2S_4)]^+$ (**3**) wherein Cp^*Ru^+ is η^5-bonded to one RhS_2C_2 ring. A third new bonding mode for TTO is illustrated by $[Cp^*_6Rh_6(C_2S_4)_2]^{4+}$, formed by the reaction of $Cp^*Rh(MeCN)_3^{2+}$ and **1**. The structure can be viewed as a dimer of **3**, except that there are no M−M bonds: the Cp^*Rh^{2+} fragments are bonded via an η^4-interaction to RhS_2C_2 rings. Furthermore, the $[Cp^*_3Rh_3(C_2S_4)]^{2+}$ subunits, which are otherwise isoelectronic with **3**, dimerize, such that all eight sulfur atoms are triply bridging.

Introduction

Tetrathiooxalate, $C_2S_4^{2-}$, and its reduced derivative ethylenetetrathiolate, $C_2S_4^{4-}$, have been the subject of intermittent study since the 1980s. Complexes of TTO are related to the metal dithiolenes,[1] e.g., they are typically electroactive with planar MS_2C_2 subunits,[2] but TTO complexes are invariably di- or polynuclear. Monometallic TTO derivatives are not known. The bridging and the electroactive characteristics of TTO are related to the semiconducting behavior of the coordination polymers $[MC_2S_4]_n$ (M = Fe, Co, Ni, Cu, Pd).[3] It is interesting to contrast the chemistry of the MTTO complexes with the corresponding oxalates, which are generally not electroactive, which do not form electrically conductive solids, and which often occur as terminal ligands.

Reflecting the bridging tendency of TTO, molecular derivatives have only been obtained through the use of strongly coordinating blocking ligands. Representative examples include $[Cp_2Ti]_2C_2S_4$,[4] $[Cp^*Ni]_2C_2S_4$,[5] $[(triphos)Rh]_2C_2S_4$,[6] and $[Ni(dithiolene)]_2C_2S_4^{2-}$.[7,8] Routes to M_2-TTO derivatives often lack generality, e.g., in situ coupling of CS_2 ligands.[4−6,9] Hoyer, however, has shown that organic salts of $C_2S_4^{2-}$ are reliable precursors to TTO complexes,[8,10−13] although this straightforward method has not been explored to any great extent by other groups. Following Hoyer's precedent, we recently prepared $Cp^*_2Rh_2Cl_2(C_2S_4)$ ($\mathbf{1}Cl_2$) by salt metathesis using $(Et_4N)_2C_2S_4$.[14] This well-behaved dirhodium species can be described as a tetrathiooxalate derivative on the basis of crystallographic criteria. This species undergoes efficient reductive dechlorination to the corresponding ethylenetetrathiolate $Cp^*_2Rh_2(C_2S_4)$ (**1**), as described in Scheme 1.

Scheme 1

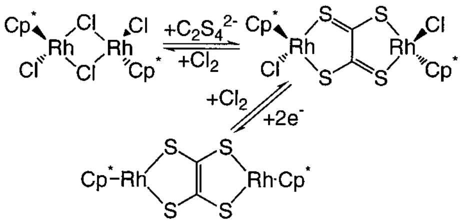

Crystallographic characterization of **1** shows that the $Rh_2C_2S_4$ core is planar; thus the extended π-system is

---

[1] (1) Mueller-Westerhoff, U. T.; Vance, B.; Wilkinson, G.; Gillard, R. D.; McCleverty, J. A. *Comp. Coord. Chem.* Pergamon: Oxford, 1987; pp 595−631.

[2] (2) Breitzer, J. G.; Chou, J.-H.; Rauchfuss, T. B. *Inorg. Chem.* **1998**, *37*, 2080−2083.

[3] (3) Reynolds, J. R.; Lillya, C. P.; Chien, J. C. W. *Macromolecules* **1987**, *20*, 1184−1191.

[4] (4) Harris, H. A.; Rae, A. D.; Dahl, L. F. *J. Am. Chem. Soc.* **1987**, *109*, 4739−4741.

[5] (5) Maj, J. J.; Rae, A. D.; Dahl, L. F. *J. Am. Chem. Soc.* **1982**, *104*, 4278−4280.

[6] (6) Bianchini, C.; Mealli, C.; Meli, A.; Sabat, M.; Zanello, P. *J. Am. Chem. Soc.* **1987**, *109*, 185−98.

[7] (7) Yang, X.; Doxsee, D. D.; Rauchfuss, T. B.; Wilson, S. R. *J. Chem. Soc., Chem. Commun.* **1994**, 821−822.

[8] (8) Pullen, A. E.; Zeltner, S.; Olk, R. M.; Hoyer, E.; Abboud, K. A.; Reynolds, J. R. *Inorg. Chem.* **1997**, *36*, 4163−4171.

[9] (9) Broadhurst, P. V.; Johnson, B. F. G.; Lewis, J.; Raithby, P. R. *J. Chem. Soc., Chem. Commun.* **1982**, 140−141.

[10] (10) Hansen, L. K.; Sieler, J.; Strauch, P.; Dietzsch, W.; Hoyer, E. *Acta Chem. Scand.* **1985**, *A 39*, 571−591.

[11] (11) Reinhold: J.; Stich, G.; Strauch, P.; Benedix, R.; Sieler, J.; Hoyer, E. *Z. Chem.* **1987**, *27*, 29−30.

[12] (12) Dietzsch, W.; Strauch, P.; Hoyer, E. *Coord. Chem. Rev.* **1992**, *121*, 43−130.

[13] (13) Pullen, A. E.; Zeltner, S.; Olk, R. M.; Hoyer, E.; Abboud, K. A.; Reynolds, J. R. *Inorg. Chem.* **1996**, *35*, 4420−4426.

[14] (14) Holloway, G. A.; Rauchfuss, T. B. *Inorg. Chem.* **1999**, *38*, 3018−9.

10.1021/om000521v CCC: $19.00

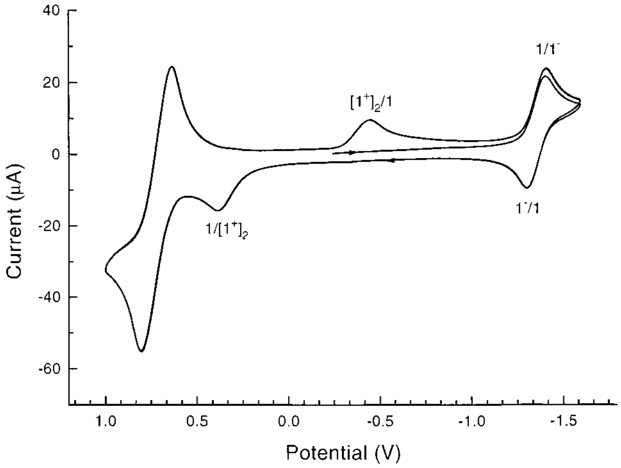

Figure 1. Cyclic voltammogram (100 mV/s) of **1** and CpFe-[$C_5H_4C(O)Me$] (internal standard) in CH_2Cl_2 solution vs Ag/AgCl at 25 °C.

exposed to attack by electrophiles. This species is therefore a promising starting point for the exploration of new C_2S_4-based complexes. Through such efforts, we have discovered three new bonding modes of the C_2S_4 ligand.

Results and Discussion

Oxidative Dimerization of Cp*$_2$Rh$_2$(C$_2$S$_4$) (1). Cyclic voltammetric (CV) measurements on **1** revealed an irreversible oxidation at 0.582 V (all potentials referenced to NHE). The return reductive sweep showed that the electro-oxidized species is reduced, again irreversibly, at −0.247 V to regenerate **1** (Figure 1). These results can be explained as follows: 1e$^-$ oxidation of **1** initially gives the unstable cation **1**$^+$. This cation undergoes dimerization to give the tetrametallic species $[Cp^*_4Rh_4(C_2S_4)_2]^{2+}$, **2** (= [**1**$^+$]$_2$). The dimerization is complete within the time scale of the CV scan (~12 s). Upon reduction of **2** at −0.247 V, the monomer **1** is regenerated as evidenced by the redox couple at −1.17 V.

To better understand the electrochemical results, we undertook the preparative-scale synthesis of **2**. Treatment of a solution of **1**, which is blue, with 1 equiv of the oxidant[15] CpFe[$C_5H_4C(O)Me$]BF_4 gave a brown solution from which we isolated the brown solid [**2**]-(BF_4)$_2$ (eq 1). Subsequent exchange of BF_4^- with BPh_4^-

$$\underset{\mathbf{1}}{2Cp^*_2Rh_2(C_2S_4)} + 2(AcFc)(BF_4) \xrightarrow{CH_2Cl_2} \underset{[\mathbf{2}](BF_4)_2}{[Cp^*_4Rh_4(C_2S_4)_2](BF_4)_2} + 2AcFc \quad (1)$$

in MeOH solution gave dark brown crystals of [**2**]-(BPh_4)$_2$. The ^1H NMR spectrum of [**2**](BPh_4)$_2$ consists of a single sharp signal in the C_5Me_5 region, consistent with a symmetric structure and a diamagnetic ground state. Integration of the C_5Me_5 peak vs the BPh_4^- signals agrees with the formula of [**2**](BPh_4)$_2$.

Complex **2** was further examined by single-crystal X-ray diffraction. In the solid state, [**2**](BPh_4)$_2$ consists of a well-separated dication, which is a dimer of **1**$^+$ (Figure 2). The two halves of the cation are linked through two pairs of Rh−S bonds such that four of the eight sulfur atoms are three-coordinate. Three distinct ranges of Rh−S bond distances are evident (Table 1). The C_2S_4 units remain planar while the Rh atoms are shifted out of the C_2S_4 planes by 0.58 Å due to interactions with the sulfur atoms in the other moiety. The C−C distance of 1.39 Å is slightly longer than that of a double bond, lying between the C−C distances found in **1**Cl$_2$ and **1**.

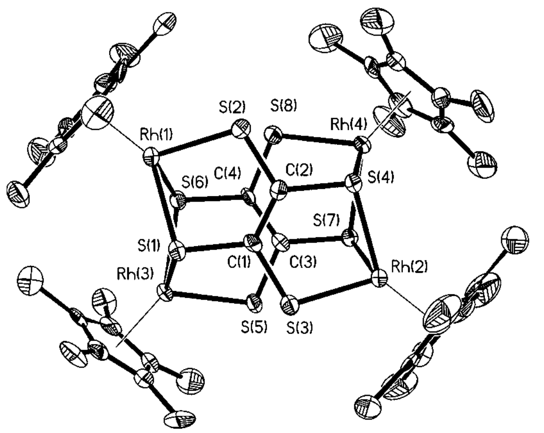

Figure 2. Structure of **2** showing 50% probability ellipsoids and atom labeling scheme.

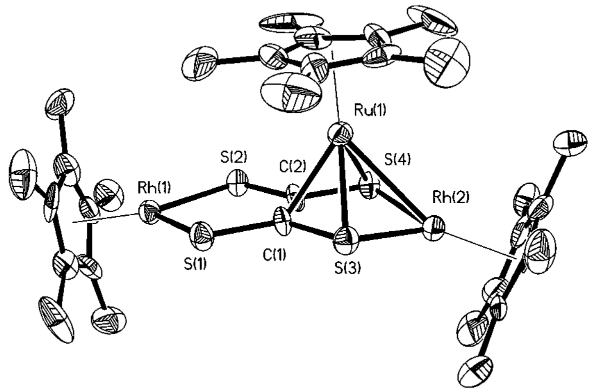

Figure 3. Structure of **3** showing 50% probability ellipsoids and atom labeling scheme.

Cp*$_2$Rh$_2$(C$_2$S$_4$) as a π-Ligand for Cp*Ru$^+$. The ability of **1** to serve as a ligand for the formation of multinuclear ensembles was investigated through its reaction with sources of the 12e$^-$ unit Cp*Ru$^+$. Treatment of solutions of **1** with [Cp*Ru(MeCN)$_3$]PF$_6$ gave purple-red $[Cp^*_3Rh_2Ru(C_2S_4)]^+$ (**3**) according to eq 2. The ^1H NMR spectrum of **3** displays three Cp* signals.

$$[Cp^*Ru(NCMe)_3][PF_6] + \underset{\mathbf{1}}{Cp^*_2Rh_2(C_2S_4)} \xrightarrow[-3\ MeCN]{CH_2Cl_2} \underset{[\mathbf{3}]PF_6}{[Cp^*_3Rh_2Ru(C_2S_4)][PF_6]} \quad (2)$$

Compound **3** was characterized by single-crystal X-ray diffraction, which revealed the structure shown in Figure 3. Crystallographic analysis of **3** shows that the connectivity of the Cp*$_2$Rh$_2$(C$_2$S$_4$) core is unmodified. The Cp*Ru$^+$ unit π-bonds to one RhS$_2$C$_2$ ring, causing that Rh to be displaced 0.34 Å from the C_2S_4 plane. The π-bonding involves an η^5-interaction, which in turn implies direct Ru−Rh bonding (2.8397 Å). The Ru−S

---

[15] Connelly, N. G.; Geiger, W. E. *Chem. Rev.* **1996**, *96*, 877−922.

Table 1. Selected Bond Lengths (Å) and Bond Angles (deg) for [2], [3], and [4]

	Bond Lengths (Å) for **[2]**		
Rh(1)−S(2)	2.296(2)	Rh(4)−S(4)	2.475(3)
Rh(1)−S(1)	2.394(2)	S(1)−C(1)	1.777(8)
Rh(1)−S(6)	2.473(2)	S(2)−C(2)	1.696(8)
Rh(2)−S(3)	2.299(2)	S(3)−C(1)	1.691(8)
Rh(2)−S(4)	2.400(2)	S(4)−C(2)	1.755(8)
Rh(2)−S(7)	2.468(2)	S(5)−C(3)	1.690(8)
Rh(3)−S(5)	2.307(2)	S(6)−C(4)	1.783(8)
Rh(3)−S(6)	2.413(2)	S(7)−C(3)	1.747(8)
Rh(3)−S(1)	2.461(2)	S(8)−C(4)	1.694(8)
Rh(4)−S(8)	2.298(2)	C(1)−C(2)	1.379)11)
Rh(4)−S(7)	2.404(2)	C(3)−C(4)	1.407(10)
	Bond Angles (deg) for **[2]**		
S(2)−Rh(1)−S(1)	86.94(8)	S(5)−Rh(3)−S(6)	86.82(8)
S(2)−Rh(1)−S(6)	97.49(8)	S(5)−Rh(3)−S(1)	96.49(8)
S(1)−Rh(1)−S(6)	77.41(8)	S(6)−Rh(3)−S(1)	77.30(8)
S(3)−Rh(2)−S(4)	86.84(8)	S(8)−Rh(4)−S(7)	86.94(8)
S(3)−Rh(2)−S(7)	96.48(8)	S(8)−Rh(4)−S(4)	97.39(8)
S(4)−Rh(2)−S(7)	77.13(8)	S(7)−Rh(4)−S(4)	76.94(8)
	Bond Lengths (Å) for **[3]**		
Rh(1)−S(1)	2.245(2)	Ru(1)−S(3)	2.380(2)
Rh(1)−S(2)	2.260(2)	Ru(1)−S(4)	2.388(2)
Rh(2)−S(3)	2.263(2)	S(1)−C(1)	1.764(7)
Rh(2)−S(4)	2.271(2)	S(2)−C(2)	1.746(8)
Rh(2)−Ru(1)	2.8397(9)	S(3)−C(1)	1.750(7)
Ru(1)−C(1)	2.223(7)	S(4)−C(2)	1.728(7)
Ru(1)−C(2)	2.263(70	C(1)−C(2)	1.423(9)
	Bond Angles (deg) for **[3]**		
S(1)−Rh(1)−S(2)	89.82(8)	S(3)−Rh(2)−S(4)	87.80(8)
	Bond Lengths (Å) for **[4]**		
Rh(1)−C(2)	2.24(3)	Rh(5)−S(3)	2.517(8)
Rh(1)−C(1)	2.26(3)	Rh(6)−S(7)	2.376(8)
Rh(2)−S(2)	2.376(8)	Rh(6)−S(8)	2.447(8)
Rh(2)−S(1)	2.394(7)	Rh(6)−S(4)	2.500(8)
Rh(2)−S(8)	2.470(7)	S(1)−C(1)	1.75(3)
Rh(3)−S(4)	2.357(8)	S(2)−C(2)	1.78(3)
Rh(3)−S(3)	2.450(8)	S(3)−C(1)	1.72(3)
Rh(3)−S(7)	2.456(7)	S(4)−C(2)	1.73(3)
Rh(4)−C(3)	2.23(2)	S(5)−C(3)	1.81(3)
Rh(4)−C(4)	2.24(2)	S(6)−C(4)	1.73(3)
Rh(4)−S(5)	2.369(8)	S(7)−C(3)	1.75(3)
Rh(4)−S(6)	2.423(8)	S(8)−C(4)	1.75(3)
Rh(5)−S(5)	2.351(8)	C(1)−C(2)	1.45(3)
Rh(5)−S(6)	2.403(8)	C(3)−C(4)	1.39(3)
	Bond Angles (deg) for **[4]**		
S(2)−Rh(2)−S(1)	78.4(3)	S(5)−Rh(5)−S(6)	77.7(3)
S(2)−Rh(2)−S(8)	85.1(3)	S(5)−Rh(5)−S(3)	85.4(3)
S(1)−Rh(2)−S(8)	97.7(3)	S(6)−Rh(5)−S(3)	98.4(2)
S(4)−Rh(3)−S(3)	87.2(2)	S(7)−Rh(6)−S(8)	86.4(2)
S(4)−Rh(3)−S(7)	80.9(3)	S(7)−Rh(6)−S(4)	79.7(3)
S(3)−Rh(3)−S(7)	99.4(3)	S(8)−Rh(6)−S(4)	101.8(2)
S(5)−Rh(4)−S(6)	77.0(3)		

distances of 2.384 Å are similar to those found in cationic thiophene complexes such as $(C_6Me_6)Ru(\eta^5\text{-}C_4R_4S)^{2+}$.[16] The Rh−S distances for the π-bonded RhS_2C_2 ring are 0.02 Å longer than the other pair of Rh−S distances on average. The C−C distance of 1.423 Å suggests multiple bonding. It is virtually impossible to distinguish Rh vs Ru by crystallographic methods, but the proposed structure is reasonable in view of the great arenophilicity of $CpRu^+$.[17] This structure is further supported by the ^{13}C NMR spectrum of this compound which shows resonances for the C_2S_4 without coupling to ^{103}Rh ($S = {}^1/_2$), thereby indicating that it is the Ru which is π-bonded to the C_2S_4.

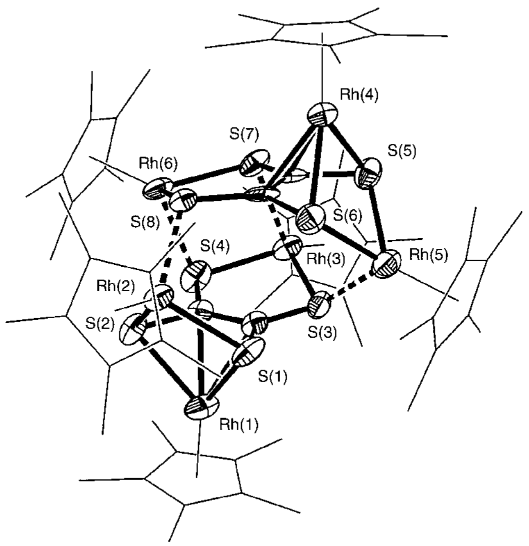

Figure 4. Structure of **4** showing 50% probability ellipsoids and atom labeling scheme. Cp* atom ellipsoids omitted and bonds between moieties shown as dotted lines for clarity.

$Cp^*_2Rh_2(C_2S_4)$ as a π-Ligand for Cp^*Rh^{2+}. In this third and final example, we investigated the binding of the dicationic $12e^-$ unit Cp^*Rh^{2+} to **1**. Treatment of a solution of **1** with 1 equiv of $[Cp^*Rh(MeCN)_3](PF_6)_2$ rapidly afforded dark purple $[Cp^*_6Rh_6(C_2S_4)_2]^{4+}$ (**4**) (eq 3). We also prepared the derivative with C_5Me_4Et in

$$2[Cp^*Rh(NCMe)_3][PF_6]_2 + \underset{\mathbf{1}}{2Cp^*_2Rh_2(C_2S_4)} \xrightarrow[-6\ MeCN]{CH_2Cl_2} \underset{\mathbf{[4]}(PF_6)_4}{[Cp^*_6Rh_6(C_2S_4)_2][PF_6]_4} \quad (3)$$

place of Cp*. ^1H NMR analysis of **4** revealed three Cp* signals, as in the case of **3**. The corresponding derivative with C_5Me_4Et in place of Cp* showed a similar pattern. The ESI-MS analysis of **4** was supportive of our assignments, showing, inter alia, a strong signal for $\{[Cp^*_6Rh_6(C_2S_4)_2](PF_6)_3\}^+$ at $m/z = 2166$.

Crystallographic analysis of **4** revealed a relatively complex hexametallic structure (Figure 4). The structure of **4** can be viewed as a dimer of the trimetallic units in **3**. In contrast to **3**, however, there are no direct M−M bonds: the additional Cp^*Rh^{2+} units in **4** are bonded via an η^4-interaction to the $Cp^*_2Rh_2(C_2S_4)$ core. Examples of η^4: η^2-dithiolene complexes are known.[18−20] In **4**, the $[Cp^*_3Rh_3(C_2S_4)]^{2+}$ subunits, which are otherwise isoelectronic with **3**, dimerize, via a pattern similar to that found in **2**. The two S atoms in the $[Cp^*_3Rh_3(C_2S_4)]^{2+}$ that are not π-bonded to the added Cp*Rh center are the atoms that bridge the two moieties. Thus, in **4**, all eight sulfur atoms are triply bridging (μ_3), each being bound to carbon and two Rh centers. As in **3**, the S_2C-CS_2 distance of 1.42 Å is between a single and a double bond distance. The C_2S_4 groups in **4** are relatively planar, but unlike the situation in **2** and **3**, one pair of

---

(16) Luo, S.; Rauchfuss, T. B.; Wilson, S. R. *J. Am. Chem. Soc.* **1992**, *114*, 8515.

(17) Fagan, P. J.; Ward, M. J.; Calabrese, J. C. *J. Am. Chem. Soc.* **1989**, *111*, 1698−1719.

(18) Lindner, E.; Butz, I. P.; Hoehne, S.; Hiller, W.; Fawzi, R. *J. Organomet. Chem.* **1983**, *259*, 99−117.

(19) Hörnig, A.; Englert, U.; Koelle, U. *J. Organomet. Chem.* **1994**, *464*, C25−C28.

(20) Rauchfuss, T. B.; Rodgers, D. P. S.; Wilson, S. R. *J. Am. Chem. Soc.* **1986**, *108*, 3114−5.

Scheme 2[a]

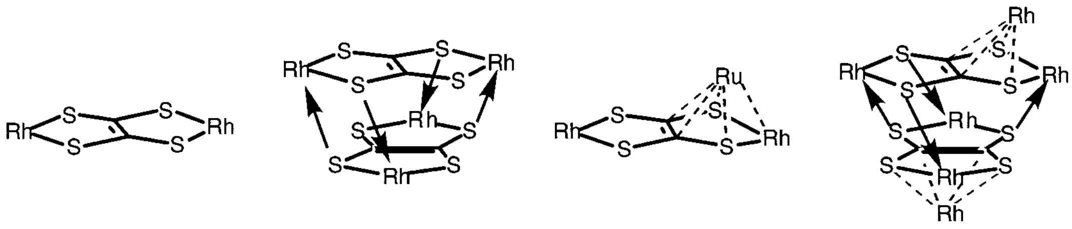

1 **2** **3** **4**

[a] Cp*'s omitted for clarity.

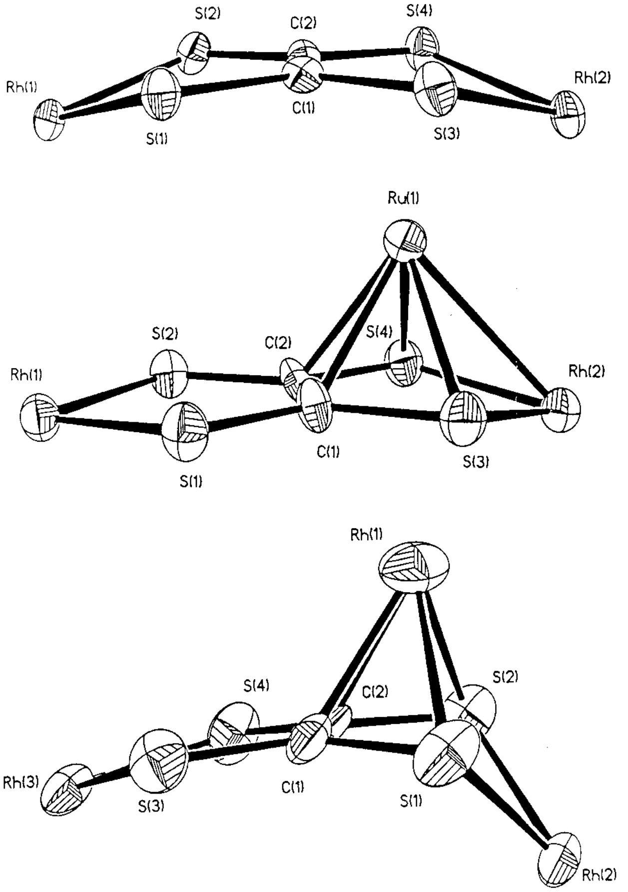

Figure 5. Partial structures of **2**, **3**, and **4** without Cp*'s showing 50% probability ellipsoids and deviation from planarity.

Rh atoms is strongly displaced (1.53 Å) from the C_2S_4 planes (Figure 5).

Summary and Conclusions

Complexes of C_2S_4 ligands have been known for many years, but there is little structural diversity in this class of compounds. Prior to our work, all C_2S_4 complexes exhibit the κ_2,κ_2-bridging interactions with the exception of $Fe_4(CO)_{12}(C_2S_4)$.[9,21] This paper demonstrates the rich structural chemistry possible for the C_2S_4 ligand; the four bonding modes are presented in Scheme 2. The results demonstrate the power of the half-sandwich organometallic reagents in exploring the chemistry of new ligands.

The trend observed in this work can be rationalized in the following qualitative but self-consistent manner. The ease of oxidation of **1** establishes its electron-rich character. As an ethylenetetrathiolato derivative, **1** is stabilized by π-donation from the negatively polarized sulfur atoms to the $16e^-$ Rh centers. When such complexes are oxidized, orbitals contract and the π-donor ability of the ethylenetetrathiolato ligand is diminished. To compensate for the weakened S to Rh π-interaction, the metal centers in $\mathbf{1}^+$ adopt a more classical structure based on σ-Rh−S interactions, which leads to dimerization of $\mathbf{1}^+$ to give **2**.

The electron-rich character of the $Rh_2C_2S_4$ core in **1** is further established by its Lewis basicity toward the Cp^*Ru^+ and Cp^*Rh^{2+} centers. In the former case, the π-interaction is equivalent to that in $Cp^*Ru(\eta^5\text{-}C_4H_4S)^+$ complexes.[22,23] In contrast, the tetracationic all-Rh derivative features no metal−metal bonding, attributable to the relatively unextended nature of the d orbitals on Rh(III). The η^4-interaction diminishes the S to Rh π-bonding within the $Rh_2C_2S_4$ core, resulting in dimerization as in the case of $\mathbf{1}^+$.

Because **2** is diamagnetic, it is clear that the odd-electron $[Cp^*{}_2Rh_2(C_2S_4)]^+$ subunits are electronically coupled. The crystallographic results show that this coupling does not occur by metal−metal bonding. The dimer structure found for **2** is relatively common for bis(dithiolene) complexes,[24] e.g., $Fe_2(mnt)_4{}^{2-}$ and $[Cp^*Rh(mnt)]_2$ (mnt = maleonitriledithiolate).[25,26] The effects that lead to dimerization are related to the ability of the dithiolene backbone to disperse charge, minimizing Coulombic repulsion, e.g., monomeric[27] $Co(S_2C_6H_3Me)_2{}^-$ vs dimeric[28] $Co_2(S_2C_6Cl_4)_4{}^{2-}$.

Experimental Section

See previous papers from this group for the description of materials and methods.[29] We previously prepared $(Et_4N)_2C_2S_4$ via our recently reported chemical synthesis.[2] Further experimentation shows, however, that electrosynthesis, originally reported in some detail by Jeroschewski,[30] is a very reliable route to gram quantities of $(Et_4N)_2C_2S_4$. The preparations of $Cp^*{}_2Rh_2Cl_4$,[31] $[Cp^*Rh(MeCN)_3](PF_6)_2$,[31] and $[Cp^*Ru(MeCN)_3]PF_6$[32] have been well described.

---

(21) Hoyer, E. *Comments Inorg. Chem.* **1983**, *2*, 261.

(22) Graf, D. D.; Day, N. C.; Mann, K. R. *Inorg. Chem.* **1995**, *34*, 1562−75.

(23) Luo, S.; Rauchfuss, T. B.; Wilson, S. R. *Organometallics* **1992**, *11*, 3497−8.

(24) Eisenberg, R. *Prog. Inorg. Chem.* **1970**, *12*, 295−369.

(25) Hamilton, W. C.; Bernal, I. *Inorg. Chem.* **1967**, *6*, 2003−2008.

(26) Don, M. J.; Yang, K. Y.; Bott, S. G.; Richmond, M. G. *J. Organomet. Chem.* **1997**, *544*, 15−21.

(27) Gray, H. B.; Billig, E. *J. Am. Chem. Soc.* **1963**, *85*, 2019−2020.

(28) Baker-Hawkes, M. J.; Dori, Z.; Eisenberg, R.; Gray, H. B. *J. Am. Chem. Soc.* **1968**, *90*, 4253−4259.

(29) Goodman, J. T.; Rauchfuss, T. B. *J. Am. Chem. Soc.* **1999**, *121*, 5017−5022.

(30) Jeroschewski, P. *Z. Chem.* **1981**, *21*, 412.

(31) White, C.; Yates, A.; Maitlis, P. M. *Inorg. Synth.* **1992**, *29*, 228−234.

Table 2. Crystallographic Data[a] for Compounds Containing [2], [3], and [4]

	[2]$(BPh_4)_2 \cdot 3CH_2Cl_2$	**[3]**PF_6	**[4]**$(BF_4)_4 \cdot 4CH_2Cl_2$
empirical formula	$C_{95}H_{106}B_2C_{16}Rh_4S_8$	$C_{32}H_{45}F_6PRh_2RuS_4$	$C_{68}H_{98}B_4C_{18}F_{16}Rh_6S_8$
formula weight	2150.24	1009.781	2420.24
crystal system	monoclinic	monoclinic	monoclinic
space group	$P2_1/c$	$C2/c$	$P2_1/c$
Z	4	8	4
a, Å	33.6441(12)	28.7077(9)	22.3241(5)
b, Å	b11.9721(4)	11.8550(6)	19.5617(2)
c, Å	26.4933(9)	22.9939(11)	21.5316(5)
α	90°	90°	90°
β	112.6430(10)°	104.806(2)°	102.6290(10)°
γ	90°	90°	90°
volume	9848.7(6) $Å^3$	7565.7 $Å^3$	9175.3(3) $Å^3$
calculated density	1.450 g/cm^3	1.773 g/cm^3	1.752 g/cm^3
absorption coefficient	1.034 mm^{-1}	1.572 mm^{-1}	1.540 mm^{-1}
θ range for data collection	1.54−25.00°	1.83−25.05°	1.40−20.00°
goodness-of-fit on F^2	1.090	1.076	1.010
final R indices[b]	$R1 = 0.0737$	$R1 = 0.0742$	$R1 = 0.0962$
$[I > 2\sigma(I)]$	$wR2 = 0.1272$	$wR2 = 0.1599$	$wR2 = 0.2337$

[a] Obtained with graphite-monochromatized Mo Kα ($\lambda = 0.71073$ Å) radiation. [b] $R1 = \Sigma||F_o| - |F_c||/\Sigma|F_o|$; $wR2 = \{\Sigma[w(F_o^2 - F_c^2)^2/\Sigma w(F_o^2)^2]\}^{1/2}$.

$Cp^*_2Rh_2Cl_2(C_2S_4)$, 1Cl_2. To a stirred slurry of 0.22 g (0.36 mmol) of $Cp^*_2Rh_2Cl_4$ in 20 mL of MeOH was added a solution of 0.17 g (0.40 mmol) of $(NEt_4)_2(C_2S_4)$[12] in 20 mL of MeOH. The slurry immediately turned from red-orange to dark green, and after ∼1 min, much precipitation appeared. After 5 min, solvent was removed under reduced pressure. The dark green solid was washed with H_2O, MeOH, and Et_2O and dried in air. Yield: 0.19 g (76%). Anal. Calcd (found) for $C_{22}H_{30}Cl_2Rh_2S_4$: C, 37.78 (37.48); H, 4.37 (4.32). ^1H NMR (500 MHz, CD_2Cl_2): δ 1.73 (Me_5C_5). ^{13}C NMR (150 MHz, CD_2Cl_2): δ 9.33 (Me_5C_5), 100.27 (Me_5C_5, $J_{Rh-C} = 6.9$ Hz), 234.71 (C_2S_4). UV−vis (CH_2Cl_2): 340, 446, 656 nm.

$Cp^*_2Rh_2(C_2S_4)$, 1. To a stirred slurry of 0.18 g (0.26 mmol) of $Cp^*_2Rh_2Cl_2(C_2S_4)$ in 30 mL of THF under an Ar atmosphere was added 0.60 mL (0.60 mmol) of a 1.0 M solution of $LiBHEt_3$ in THF. After ∼1 min, the slurry turned from dark green to dark blue. Solvent was removed under reduced pressure to ∼5 mL after 7.5 h. Addition of 50 mL of hexane precipitated a dark blue solid, which was washed with 5 × 10 mL of MeOH and 10 mL of Et_2O. Yield: 88 mg (55%). Anal. Calcd (found) for $C_{22}H_{30}Rh_2S_4$: C, 42.04 (41.85); H, 4.81 (4.85). ^1H NMR (500 MHz, CD_2Cl_2): δ 1.95 (Me_5C_5). ^{13}C NMR (150 MHz, CD_2Cl_2): δ 10.79 (Me_5C_5), 97.37 (Me_5C_5, $J_{Rh-C} = 6.9$ Hz), 169.45 (C_2S_4). UV−vis (CH_2Cl_2): 688 nm.

$[Cp^*_4Rh_4(C_2S_4)_2](BF_4)_2$, 2$(BF_4)_2$. A dark blue solution of 0.0541 g (0.086 mmol) of **1** in 15 mL of CH_2Cl_2 was added to a dark blue solution of 0.0271 g (0.086 mmol) of $\{[CH_3C(O)C_5H_4]Fe(C_5H_5)\}BF_4$[15] in 15 mL of CH_2Cl_2, resulting in an immediate color change to dark brown. After 30 min, no further color change was apparent and solvent volume was reduced in vacuo to ∼5 mL. Addition of 100 mL of dry, degassed Et_2O yielded a dark brown solid, which was collected by filtration, washed with Et_2O, and dried in air. Yield: 0.0536 g (87%). Anal. Calcd (found) for $C_{44}H_{60}B_2F_8Rh_4S_8$: C, 36.94 (36.69); H, 4.23 (4.21). ^1H NMR (500 MHz, CH_2Cl_2): δ 1.76. UV−vis (CH_2Cl_2): 380, 416, 516 nm. ESI-MS: 1343 ($[Cp^*_4Rh_4(C_2S_4)_2](BF_4)^+$).

$[Cp^*_4Rh_4(C_2S_4)_2](BPh_4)_2$, 2$(BPh_4)_2$. A solution of 0.017 g (0.05 mmol) of $NaBPh_4$ in 5 mL of MeOH was added to a dark brown solution of 0.0215 g (0.02 mmol) of **2**$(BF_4)_2$ in 10 mL of MeOH. A brown precipitation appeared immediately. The reaction was filtered and washed with 2 × 20 mL of H_2O and 3 × 20 mL of Et_2O and dried in air. Yield: 0.229 g (92%). ^1H NMR (500 MHz, CD_3CN): δ 7.3 (16 H), 7.0 (16 H), 6.8 (8 H), 1.71 (59 H).

$[Cp^*_3Rh_2Ru(C_2S_4)]PF_6$, 3$PF_6$. To a yellow slurry of 0.0406 g (0.080 mmol) of $[Cp^*Ru(CH_3CN)_3]PF_6$ in 10 mL of CH_2Cl_2 was added a dark blue solution of 0.0506 g (0.080 mmol) of **1** in 15 mL of CH_2Cl_2, resulting in a dark purple-red solution within a few minutes. After 2 h, 10 mL of hexanes was added to the reaction, and the solvent volume was reduced to about 10 mL under reduced pressure. A dark purple crystalline solid was collected and washed with Et_2O and dried in air. Yield: 0.0670 g (84%). Anal. Calcd (found) for $C_{32}H_{45}F_6PRh_2RuS_4$: C, 38.06 (37.66); H, 4.49 (4.40). ^1H NMR (500 MHz, CH_2Cl_2): δ 1.95, 1.87, 1.61 (equal intensity singlets for Cp*'s). ^{13}C NMR (750 MHz, CD_2Cl_2): δ 10.5, 10.7, 11.2 (C_5Me_5); 94.3 (s), 99.7 (d), 100.0 (d) (C_5Me_5); 127.9 (s) (C_2S_4). UV−vis (CH_2Cl_2): 446, 590 nm. FAB-MS: 865.1 ($[Cp^*_3Rh_2Ru(C_2S_4)]^+$).

$[Cp^*_6Rh_6(C_2S_4)_2](PF_6)_4$, 4$(PF_6)_4$. A mixture of 0.0231 g (0.035 mmol) of $[Cp^*Rh(CH_3CN)_3](PF_6)_2$ and 0.0217 g (0.035 mmol) of **1** was dissolved in 35 mL of CH_2Cl_2 to give a dark red solution. After 2 h of stirring, the reaction was filtered through Celite in air, and the filter cake was washed with CH_2Cl_2. The red filtrate was diluted with 20 mL of hexanes, and the solution volume was reduced in vacuo to ∼10 mL to give purple-black crystals. Yield: 0.0288 g (72%). Anal. Calcd (found) for $C_{64}H_{90}F_{24}P_4Rh_6S_8$: C, 33.23 (33.62); H, 3.92 (3.94). ^1H NMR (500 MHz, CD_2Cl_2): δ 2.07, 1.96, 1.75 (equal intensity singlets for Cp*'s). UV−vis (CH_3CN): 262, 388, 534 nm. ESI-MS: 2166 ($[\mathbf{4}(PF_6)_3]^+$), 867 ($[Cp^*_3Rh_3(C_2S_4)]^+$), and 433 ($[Cp^*_3Rh_3(C_2S_4)]^{2+}$).

Crystallographic Analysis of 2. The data crystal, a red plate, was mounted using Paratone oil with the (1 0 1) scattering planes roughly normal to the spindle axis. Data were collected on a Siemens Smart CCD detector using a 0.25°/s ω scan width and a 0.333 s scan time. Of 51 660 reflections collected for θ ranging from 1.54 to 25.00°, 17 327 were independent with $R_{int} = 0.1086$, after Platon Squeeze removed two CH_2Cl_2 solvent molecules. Details of the crystal data and refinement are given in Table 2.

The structure was solved by direct methods and refined using the SHELX suite of programs.[33−35] The initial solution located the C, S, and Rh atoms of the cationic core as well as some of the Cp* C atoms and most of the BPh_4^- atoms. Further refinement cycles allowed the location of the rest of the atoms as well as the presence of solvent molecules. All nonsolvent molecules were refined anisotropically. The largest residual peak (0.86 $e^-/Å^3$) was located 0.973 Å from Rh4. All Cp* rings were refined as variable metric rigid groups.

Present in the asymmetric unit were three molecules of CH_2Cl_2. The first (C93) was ordered and refined anisotropically.

---

(32) Steinmetz, B.; Schenk, W. A. *Organometallics* **1999**, *18*, 943−6.

(33) Sheldrick, G. M., SAINT v5 and SHELXTL v5, Bruker AXS, 1998.

(34) Sheldrick, G. M., SHELXS 86, University of Gottingen, 1986.

(35) Sheldrick, G. M., SHELXL-97, University of Göttingen, 1997.

The other two (C94 and C96) were each disordered over two positions with occupancies of 50/50 for the C94/C95 pair and 80/20 for the C96/C97 pair. Also present were an additional two highly disordered CH_2Cl_2 molecules. Because of the high disorder and overlapping positions of these two solvent molecules, Platon-99 was used to remove the electron density due to these molecules.

Crystallographic Analysis of 3. The data crystal, a dark red plate, was mounted using Paratone oil with the (0 1 0) scattering planes roughly normal to the spindle axis. All crystals examined were severely twinned with a pseudo mirror normal to the *a*-axis. Two orientations were measured and integrated for the data crystal. Intensities were corrected for absorption by integration and then filtered by position and relative intensity to omit partially overlapped data. Data were collected on a Siemens Smart CCD detector using 0.25° ω frames scanned for 20 s per frame. A total of 26949 reflections were collected from both orientations for θ ranging from 1.5 to 25.0°. Details of the crystal data and refinement are given in Table 2.

The structure was solved by direct methods and refined using the SHELX suite of programs.[33−35] The initial solution allowed the location of the atoms of the PF_6^- anion and the cationic core with the exception of some of the Cp* C atoms. Further refinement cycles allowed the location of the rest of the atoms. The largest residual peak (1.73 $e^-/Å^3$) was located 1.6 Å from a methyl hydrogen on C32. All non-H atoms were refined anisotropically. The Cp* rings were refined as variable metric rigid groups.

Crystallographic Analysis of 4. The data crystal, a red plate, was mounted using Paratone oil with the (1 2 0) scattering planes roughly normal to the spindle axis. Data were collected on a Siemens Smart CCD detector using 0.3°/s ω scan width and a 0.333 s scan time. A total of 29 903 reflections were collected for θ ranging from 1.40 to 20.00°, 8548 were independent with $R_{\text{int}} = 0.1941$. Details of the crystal data and refinement are given in Table 2.

The structure was solved by direct methods and refined using the SHELX suite of programs.[33−35] The initial solution allowed the location of the C, S, and Rh atoms of the cationic core with some of the Cp* C atoms and two of the BF_4^- anions. Further refinement cycles allowed the location of the rest of the atoms as well as two more anions and solvent molecules. One reflection (1 1 0) was omitted due to being truncated by the beamstop. The largest residual peak (3.58 $e^-/Å^3$) was located 1.683 Å from Rh1.

All Cp* rings were refined isotropically as fixed groups. The Cp* bound to Rh1 was disordered 53/47 over two orientations. The isotropic displacement parameter for all carbon atoms of the disordered Cp* were restrained to be equal.

Four molecules of BF_4^- are present in the asymmetric unit. Only one (B1) is ordered. The other three are disordered over two positions with occupancies of 66/34 for the B2/B2′ pair, 70/30 for the B3/B3′ pair, and 56/44 for the B4/B4′ pair. Because of the poor quality data, all of the BF_4^- counterions were refined isotropically and the isotropic displacement parameter was restrained to be equal for all atoms of each ion/disordered pair. The B−F bond length was restrained to 1.365(1) Å.

Also present are four molecules of CH_2Cl_2 solvent. Only one of these (C70) was not disordered. Two of the other solvent molecules were disordered over two positions with occupancies of 77/24 for the C65/C66 pair and 70/30 for the C71/C72 pair. The remaining CH_2Cl_2 was disordered over three positions with occupancies of 42/48/10 for the C67/C68/C69 set. Because of the poor quality of the data set, all solvent molecules were refined isotropically and the isotropic displacement parameter was restrained to be equal for equivalent atoms of each molecule/disordered set. The C−Cl bond length was restrained to 1.779(1) Å and the Cl−Cl distance was restrained to 2.994(1) Å.

Acknowledgment. This research was supported by the Department of Energy through DEFG02-96ER45439 and by NSF. G.A.H. is supported through a Hertz Fellowship.

Supporting Information Available: Tables of atomic coordinates, selected bond distances and angles, and thermal parameters. This material is available free of charge via the Internet at http://pubs.acs.org.

OM000521V